De novo origin of multicellularity in response to predation

Matthew D. Herron[1,2], Josh M. Borin[2], Jacob C. Boswell[1,2], Jillian Walker[2], Charles A. Knox[1], Margrethe Boyd[1], Frank Rosenzweig[1,2], and William C. Ratcliff[2]

1. University of Montana, Division of Biological Sciences, Missoula, MT

2. Georgia Institute of Technology, School of Biological Sciences, Atlanta, GA

Corresponding author: Matthew D. Herron, xprinceps@gmail.com

Abstract

The transition from unicellular to multicellular life was one of a few major events in the history of life that created new opportunities for more complex biological systems to evolve. However, understanding the proximate and ultimate causes of the resulting increases in complexity remains a major challenge for evolutionary biology. Questions related to the emergence of multicellularity have traditionally been addressed through retrospective, comparative studies of extant unicellular and multicellular lineages. Experimental microbial evolution allows prospective studies that observe evolution in real time. We have generated a *de novo* origin of simple multicellularity in response to predation. We subjected outcrossed populations of the unicellular green alga *Chlamydomonas reinhardtii* to selection by the filter-feeding predator *Paramecium tetraurelia*. Two of five experimental populations evolved multicellular structures not observed in any of the three unselected control populations within ~300 asexual generations. Considerable variation exists in the evolved multicellular life cycles, with both cell number and propagule size varying among isolates. Survival assays show that multicellularity provides some protection against predation. These results support the hypothesis that selection imposed by predators may have played a role in some origins of multicellularity.

Introduction

Nearly all macroscopic life is multicellular. As Leo Buss pointed out in *The Evolution of the Individual*, the very existence of integrated multicellular organisms is an outcome of evolutionary processes, not a starting condition (Buss 1987). It seems, in fact, to be a common outcome: multicellular organisms have evolved from unicellular ancestors dozens of times (Bonner 1998; Kaiser 2001; Grosberg and Strathmann 2007). Animals, land plants, fungi, red algae, brown algae, several groups of green algae, cellular and acrasid slime molds, and colonial ciliates, among others, each descend from a different unicellular ancestor (Grosberg and Strathmann 2007; Herron et al. 2013).

Each of these independent transitions to multicellular life is a replicate experiment with the potential to illuminate the ways and reasons that multicellularity has evolved. In the broadest terms, two approaches have proven valuable in exploiting that potential. The fossil record, when stratigraphically calibrated, can not only reveal what nascent multicellular organisms looked like, but can set limits on when they evolved. For example, the red algal fossil *Bangiomorpha* showed that multicellular red algae evolved at least 1.2 billion years ago and that early multicellular red algae had both sexual reproduction and cellular differentiation (Butterfield 2000).

Comparative approaches, including morphological, developmental, and genetic and genomic comparisons, have proven valuable in reconstructing changes associated with the evolution of multicellularity. Comparisons between animals and our closest unicellular relatives, for example, suggest that protein families used for cell signaling and cell adhesion in animals originated in our unicellular ancestors (King et al. 2003).

Although both of these retrospective approaches have been critical to our understanding of early multicellular evolution, each has its limitations. Fossils like *Bangiomorpha* are very much the exception; for most multicellular groups, little or no fossil evidence exists that is relevant to the first steps in the transition from unicellular to multicellular life. Comparative methods suffer from a lack of intermediate forms between the multicellular organisms we are interested in and their extant unicellular relatives. Furthermore, direct knowledge of unicellular ancestors is not available. Extant unicellular relatives often serve as stand-ins, but this is a poor approximation, as they have been evolving independently since they diverged from their multicellular relatives.

A third, prospective, approach designed to circumvent these limitations has emerged in the last decade. The experimental evolution of multicellularity in otherwise unicellular microbes enables real-time observations of morphological, developmental, and genetic changes that attend the transition to multicellular life. Boraas and colleagues exposed cultures of the green alga *Chlorella vulgaris* to predation by the flagellate *Ochromonas vallescia*, resulting in the evolution of small, heritably stable algal colonies (Boraas et al. 1998). Becks and colleagues showed that exposure to the predatory rotifer *Brachionus calyciflorus* selected for heritable changes in the rate of formation of multicellular palmelloids in the green alga *Chlamydomonas reinhardtii* (Becks et al. 2010). And Ratcliff and colleagues have shown that selection for an increased rate of settling out of liquid suspension consistently results in the evolution of multicellular 'snowflake' colonies in the yeast *Saccharomyces cerevisiae* (Ratcliff et al. 2012). Predation has long been hypothesized as a cause for the evolution of multicellularity, as most predators can only consume prey within a narrow range of sizes (e.g., Stanley 1973;

Bell 1985; Bonner 1998; Pentz et al. 2015). Filter-feeding predators are common in aquatic ecosystems, and algae that are larger than a threshold size are largely immune to them (Bell 1985). Predation is thus ecologically plausible as an explanation for at least some origins of multicellularity.

In this study, we describe experiments in which we used the ciliate predator *Paramecium tetraurelia* to select for the *de novo* evolution of multicellularity in outcrossed populations of *C. reinhardtii*. We present qualitative and quantitative descriptions of the multicellular life cycles that evolved and compare them to the ancestral, unicellular life cycle. In addition, we show that the evolved multicellular phenotype provides a viability advantage in the presence of predators. Because *C. reinhardtii* has no multicellular ancestors, these experiments represent a completely novel origin of multicellularity (Herron and Michod 2008; Leliaert et al. 2012).

Methods

Experimental evolution

To increase genetic diversity at the onset of the experiment, we founded five experimental and three control populations from an F1 cross. We obtained plus (CC-1690) and minus (CC-2290) mating type strains of *C. reinhardtii* from the *Chlamydomonas* Resource Center (www.chlamycollection.org) and crossed them using a protocol adapted from Harris (2009). Vegetative cells were grown to high density in 10 mL TAP medium (Gorman and Levine 1965) at 22.5°C and pelleted in 15 mL conical tubes by centrifugation for 5 min. at 2000 × *g*. Pelleted cells were resuspended in 10 mL mating medium (TAP minus NH_4Cl) and grown in light for 6 h to induce gametogenesis. Gametes were mixed in a 24-well tissue

culture plate, 0.5 mL of each mating type, and incubated in light for 4 h and dried in the dark. Single mating-type controls of 1 mL were treated identically to ensure that no vegetative material survived desiccation. After 20 days in the dark, crosses and single mating-type controls were each flooded with 1 mL TAP medium and placed in light at 22.5°C to germinate. Single mating-type controls showed no evidence of vegetative growth after two weeks; thus, desiccation was effective in killing vegetative material and surviving algae from the crosses must be outcrossed.

Experimental populations were started by mixing 0.1 mL of *C. reinhardtii* F1 cultures, grown to ~2×10^6 cells/mL, with 0.1 mL of a culture of *P. tetraurelia*, grown to ~2×10^5 cells/mL, in 1.3 mL of COMBO medium (Kilham et al. 1998), making a final volume of 1.5 mL. Control populations were founded by inoculating 0.1 mL of *C. reinhardtii* F1 cultures in 1.4 mL of COMBO medium. All populations were propagated in 24-well plates and transferred weekly.

During transfers, populations were homogenized with a multichannel pipette by drawing and dispensing 1 mL three times. After mixing, 0.1 mL of culture was transferred to 1.4 mL fresh COMBO in a new 24-well plate.

After 50 weeks, populations were plated on TAP medium + 1.5% agar. For each population plate, eight individual colonies were randomly picked and re-plated on agar. Individual colonies were picked and re-plated a minimum of three times each, to ensure that each was free of contaminants and was purely clonal.

We performed an initial characterization of evolved phenotypes using light microscopy. A homogenized dilution of each isolate grown in TAP medium was fixed in iodine and stored at 4°C. For each isolate, 48 µL samples were photographed in replicate

on a hemocytometer. Images for each of the clones were processed in ImageJ to determine particle counts and relative particle sizes, and these data were later processed in Python to determine the relative proportions of different sized particles. The size threshold used to distinguish between unicellular and multicellular particles was user-determined and was rarely violated by any samples. In instances where the size threshold was violated, small multicellular particles were counted as unicells and not the other way around.

Maximum Cells Per Cluster

To determine the maximum cells per cluster of evolved *C. reinhardtii* strains, cells were stained and imaged via fluorescent microscopy over a 6-day examination period. Genetic analyses were used to determine which single strain isolates were unique from each evolved population, as some strains from a given population were genetically identical (Chen et al. unpublished data). Eight single strain isolates from the B2 predation-selection treatment, two strains from the B5 predation-selection treatment, and two strains from the control treatment (K1) were chosen for all analyses hereafter.

Strains were cultured in 10 mL of TAP medium (Harris 2009) in a climate-controlled chamber on a 14/10-hour light/dark cycle (23.5ºC, 41% humidity, 326 lx). In order to standardize starting cell concentrations, preliminary cultures were first inoculated from scrapes of colonies on TAP agar plates and allowed to grow, without disruption, for 6 days until reaching stationary phase. Cultures were then transferred 1:100 into fresh TAP medium and examined over a following 6-day examination period.

Throughout the examination period, cultures were sampled, stained, and imaged every 12 hours in order to capture the maximum size attained by various strains before reaching stationary phase. Strains B5-05 and B5-06 were not sampled at the final timepoint. Samples were extracted from well-mixed culture tubes and transferred into 1.5 mL microcentrifuge tubes (200 μL from the first 6 timepoints to compensate for low cell density, 100 μL from all timepoints thereafter). The samples were centrifuged at 250 x g for 5 minutes and the supernatant was replaced by a 50% v/v ethanol-water solution to fix cells and make cell membranes more permeable to the DAPI (4',6-diamidino-2-phenylindole) fluorescent nucleotide stain. After waiting 10 minutes for the ethanol to fix cells, samples were centrifuged again (250 x g for 5 minutes) and the supernatant was replaced with distilled water containing 1 μg/mL DAPI. Cells with DAPI were kept in darkness for one hour and then moved to a refrigerator without light to prevent photo bleaching until imaging on the microscope

Prior to imaging, samples were removed from the refrigerator and inverted to mix cultures. Seven μL of each sample was mounted on glass microscope slides and large 6 × 6 images were stitched from individual images captured at 40x magnification, creating high-resolution (441 megapixel) wide-field images, providing a robust measurement of the distribution of clusters sizes within the population.

Image and data analysis

Large stitched images of individual samples were imported and analyzed in Fiji (Schindelin et al. 2012). We wrote and implemented a script in ImageJ macro (Supplemental Material) to automatically calculate the number of cells in each cluster. The script did this by

demarcating cluster boundaries and recording the number of pixel maxima within each boundary, corresponding to the number of DAPI-stained nuclei. Following this procedure, all images used in our analyses were manually screened and any region of interest resulting from artifacts (*e.g.,* dust particles, autofluorescence) were removed from the dataset. Data for five technical replicates of all 12 strains, each represented by 12 time-points sampled over six days, were concatenated into one large dataset.

In order to determine the maximum number of cells per cluster for each strain, hereafter referred to as "cluster size," we first determined the time-point at which clusters were largest. This was calculated separately for each strain, as different strains reached their maximum size at different time-points during the six-day culture cycle. First, we calculated the median cluster size of each replicate and at each time-point throughout the culture cycle, which better represented the central tendency than the mean, as the distributions of cluster sizes were right-skewed and occasionally contained large outliers.

To determine the time-point at which cluster size was largest for each strain, we calculated the average of the median cluster size from replicate populations within each time-point. The first time-point, representing cluster sizes at time of inoculation, was removed from analysis.

Number of Cells per Propagule

In order to determine the number of cells per propagule released by clusters of each strain, hereafter referred to as "propagule size," we time-lapse imaged all strains over 72 hours of growth. First, cells were inoculated from colonies on plates into liquid culture and incubated for five days to grow to high density. Then, each culture was homogenized by

vortexing and was transferred 1:100 into five replicate tubes of fresh TAP medium and allowed to grow for two days. Two day old cultures were mixed by vortexing, diluted 1:10 in TAP medium, and then 100 μL from each culture was randomly inoculated into the central 60 wells of a 96-well plate that already contained 100 μL of TAP medium in each well.

For time-lapse microscopy, the 96-well plate (containing five technical replicates of each of the 12 strains) was imaged at 20x magnification, where the field of view was positioned on cells near the center of the well. The time-lapse was run for 72 hours, capturing images of each well every 30 minutes.

Time-lapse images were manually analyzed using ImageJ. For each well, all images from the time-lapse were viewed individually and sequentially. All cells or clusters of cells in the frame at the beginning of the time-lapse were labeled with a number indicating their identity. Throughout the time-lapse, when a cell or cluster of cells was seen to separate from the initial parental cluster/group, the number of cells in the propagule was recorded. For wells that had few or no initial cells in the frame (typically occurring for motile, unicellular strains), cells or clusters of cells were labeled as they entered the field of view, until collecting a sufficient sample size ($N > 5$ parental clusters). Due to the long time required for clusters to fully separate physically, even after they have detached from a parent cluster, propagule sizes were recorded four frames (two hours) after the propagule was observed to initially split from the parental cluster. Time lapse data were analyzed in R (R Development Core Team 2009).

Defense against predators

To test whether multicellularity affords protection from predators, we subjected evolved unicellular and multicellular isolates to predation by the rotifer *Brachionus calyciflorus*. Rotifers were obtained as cysts in vials and stored at 4°C in the dark. To ensure a contaminant-free culture of *B. calyciflorus*, cysts were treated and incubated according to the protocol described by Suga *et al*. (2011). Neonate rotifers were grown axenically in 10 mL of WC medium (Guillard 1975) with 100 µg/mL ampicillin in culture tubes at the same temperature and light conditions as the *C. reinhardtii* cultures. In order to sustain the population of *B. calyciflorus* before the experiment, 1.0 mL of an axenic strain of *C. reinhardtii*, CC-1690, was inoculated into the culture via micropipette.

Evolved isolates of *C. reinhardtii* were grown to high density; cultures' absorbance was estimated using a microplate reader (Molecular Devices SperctraMax® M5, 420 nm), whereafter each was diluted to approximately 3.45×10^5 cells/mL. Four replicates of each strain were randomly assigned to 24-well plates and 1.33 mL of each strain pipetted into a designated well according to a randomized design so as to negate any potential plate effects. Rotifer cultures were poured through a 25 μm mesh filter to remove the algae they had been feeding on, then pipetted into a sterile test tube awaiting transfer to the experimental wells (*C. reinhardtii* cells are ~10 μm in diameter and easily pass through the filter). Depending on the treatment condition, 0.67 mL of either growth medium or predator culture was added to each well. After an initial density reading, the plates were stored in an incubator under lights in 14:10 diurnal cycle at 22.5 °C for 5 days. Throughout the 14-hour light period, absorbance readings were taken every 3 hours, providing a high-resolution picture of the growth rate for all strains.

Results

Response to Selection

After 50 weekly transfers (~750 generations), simple multicellular structures evolved in two of five predation-selection treatments (Populations B2 and B5). Such multicellular structures were not observed in any of the control populations. Eight strains were isolated from each of three populations (B2, B5, K1). We focused our analyses on eight strains from B2 (B2-01, B2-03, B2-04, B2-06, B2-07, B2-10, B2-11, B2-12) and two strains from B5 (B5-05, B5-06). Of the isolates from the control population that evolved in the absence of predators (K1), we analyzed two strains (K1-01, K1-06). Because strains maintained their characteristics of simple multicellularity for four years as unfrozen, in-use laboratory strains, we are confident that the phenotypic traits we report are stable and genetically linked. We consider the aforementioned strains below.

Some clones, notably those in population B5, commonly formed stereotypic eight-celled clusters, with an apparent unicellular and tetrad life stage (Fig. 1A). Other clones, notably those in population B2, appeared to form amorphous clusters of unpredictable cell number, with varying degrees of unicellularity present (Fig. 1B). Other phenotypic differences could be easily discerned by light microscopy. For example, in Fig. 1, an external membrane is visible around both evolved multicells, indicating that they formed clonally via repeated cell division within the cluster, rather than via aggregation.

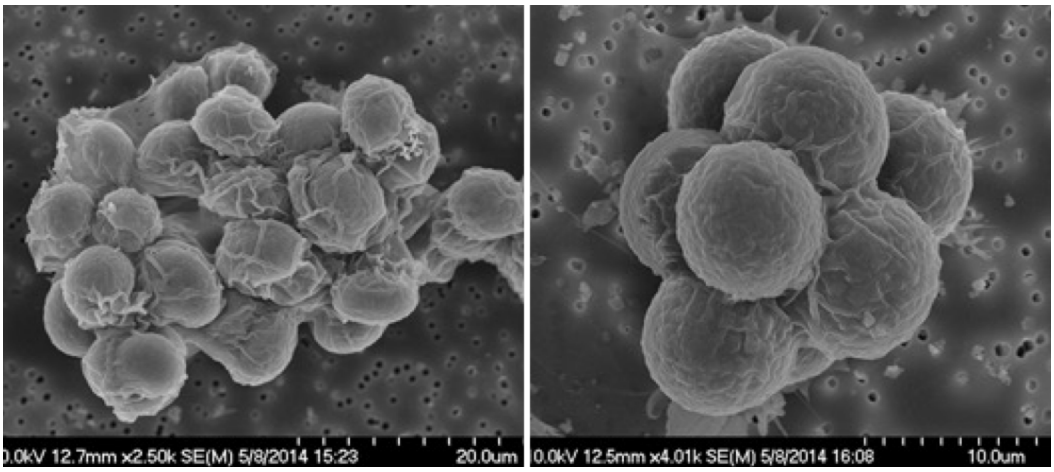

Figure 1. Scanning electron micrographs of representative multicells from evolved populations. [A] shows an amorphous cluster from population B2. Cell number varies greatly between clusters in this clone and between clones in this population. [B] shows an eight-celled cluster from population B5. Octads were frequently observed both in this clone and in other clones from the same population.

Life Cycles

We found a variety of life cycles within and among populations. Using time-lapse videos of evolved strains growing in liquid culture in 96-well tissue culture plates, we qualitatively classified strains into five life cycle categories to compare their similarities and differences (Fig. 2A-E). We discuss each life cycle category below, and then present quantitative measurements on parent and propagule cluster sizes.

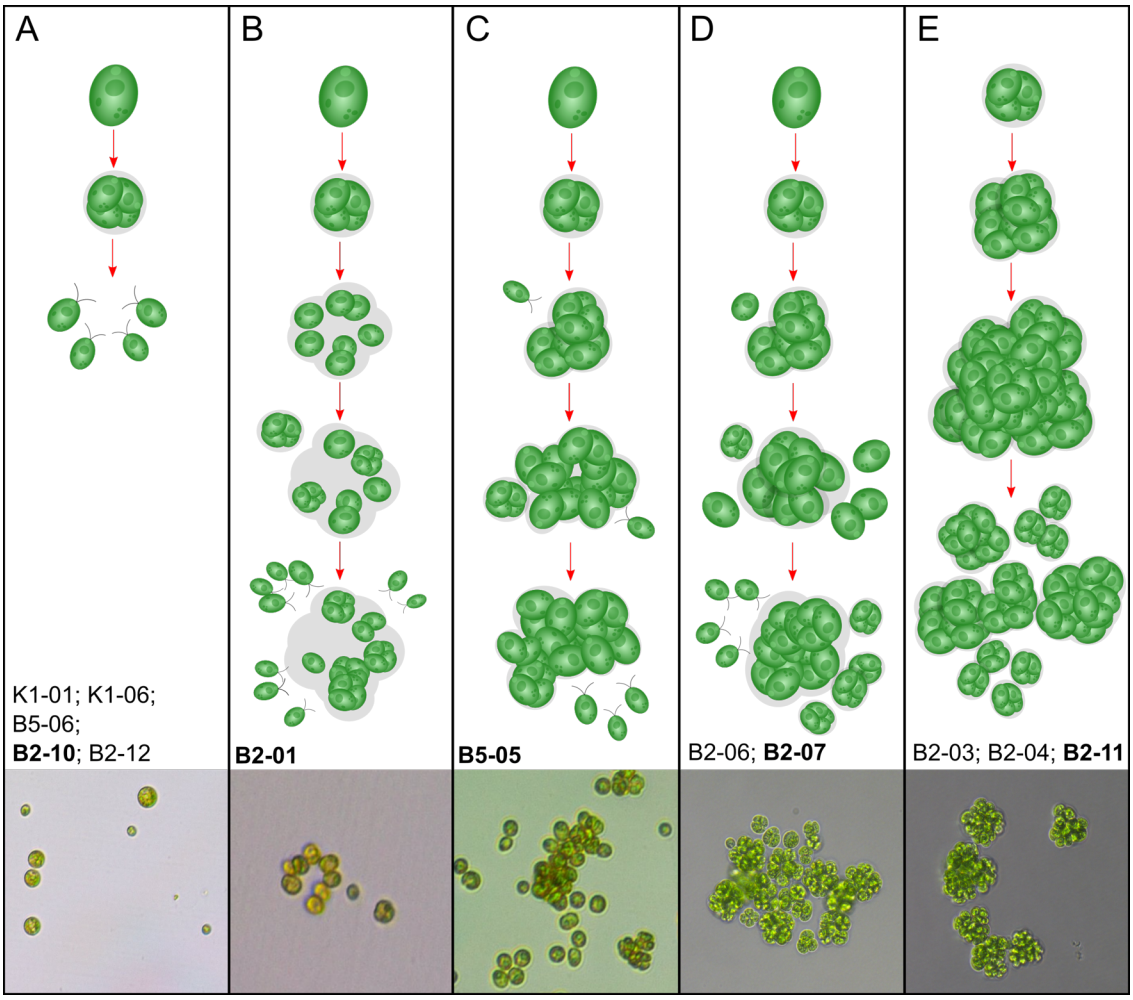

Figure 2. Depiction of *C. reinhardtii* life cycles following evolution with or without predators for 350 days. Categories (A-E) show a variety of life cycle characteristics, from unicellular to various multicellular forms. Evolved strains were qualitatively categorized based on growth during 72-hour timelapse videos. Strains within each life cycle category are listed below the drawings. Representative images of each category are at the bottom (Depicted strain in bold). Strains from the B2 and B5 populations evolved with predators. Strains from the K1 population evolved without predators.

In population K1, which evolved without predators, ancestral life cycle characteristics of the unicellular, wild type *C. reinhardtii* were retained (Fig. 2A). Specifically, as cells reproduce asexually, they lose motility and undergo 2-5 rounds of mitosis before releasing motile, single-celled propagules. It should be noted that even in wild-type *C reinhardtii*, the dividing parent cluster is a *transient* multicellular stage, but

does not persist after propagules are released. Interestingly, in the two populations that evolved multicellularity in response to predation (B2, B5), strains B2-10, B2-12, and B5-06 retained a life cycle typical of the ancestral, wild type *C. reinhardtii*.

Life cycles of the remaining strains isolated from populations B2 and B5 were distinct from the ancestor, as clusters of various sizes persist through multiple rounds of reproduction. Ordinarily, strain B2-01 releases motile, single-celled propagules during reproduction, similar to the ancestor. However, in some clusters, cells undergoing division separate, but remain proximately located because they are embedded in an extracellular matrix (ECM) of the parent cluster (Fig. 2B). As these cells continue to grow and divide, some remain embedded in the ECM, which creates growing aggregations of cells. Strain B5-05 also produces motile, single-celled propagules that are often embedded in the maternal ECM. In addition to retaining propagules embedded in the ECM, growing clusters of B5-05 ensnare free-swimming cells, which create aggregations that grow much larger than those of B2-01 (Fig. 2C).

Conversely, five of the strains isolated from population B2 exist in cell clusters comprised only of direct descendants, as opposed to chimeric aggregations with free-swimming cells. Cells growing in strains B2-06 and B2-07 remain tightly associated within the mother cell wall (Fig. 2D). Propagules are released as small clusters or single cells that immediately undergo cell division (Supplemental Video 1). Although the majority of propagules are immobile, some single-celled propagules are motile. Similarly, clusters from strains B2-03, B2-04, and B2-11 grow in tightly associated groups of direct descendants embedded in the maternal cell wall (Fig. 2E). However,

propagules of these strains are typically larger and, critically, no motile propagules were observed throughout the 72-hour timelapse video.

Average Maximum Cells Per Cluster

In order to determine the size attained by evolved strains, we sampled, stained, and imaged growing cultures in tubes every 12 hours over a 6-day period. We find that cluster sizes of strains that evolved without predators (K1-01, K1-06) and strains that retained ancestral life cycle traits, despite evolving with predators (B5-06, B2-10, B2-12), remain small throughout the six days of growth (Fig. 3). Even at their largest, the mean of replicate population median sizes for strains K1-01 and K1-06 was one cell per cluster, showing that these strains exist as unicellular individuals with transient multicellular forms at reproduction. Similarly, we find that cells of strain B2-01 exist primarily as single cells, with a mean of median sizes of 1.8. It is possible that clusters of this strain, which separate from contact within the maternal ECM/cell wall during reproduction, were dispersed during procedures to stain and image cells. The mean of median sizes of strain B5-05 was 4, larger than strains that retained the ancestral phenotype and B2-01. Unlike strains B2-01 and B5-05, in which ECM holds cells in clusters, cells of the largest strains are primarily encapsulated within the mother cell wall. Means of medians for these strains (B2-06, B2-07, B2-11, B2-03, and B2-04) were 7.8, 5.4, 6.2, 6.2, and 5.6, respectively.

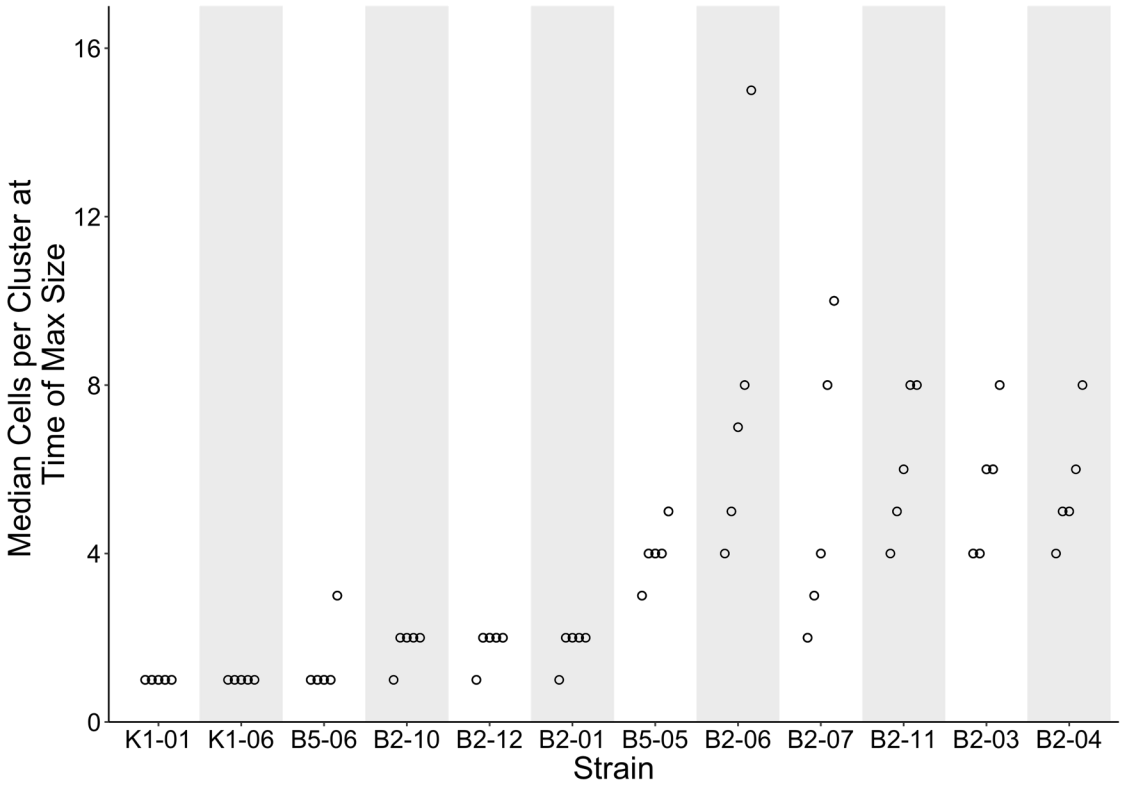

Figure 3. Median cluster sizes of evolved strains at the time-point where strains reached maximum size. To determine the time where strains were largest, we calculated the mean from five replicate medians (open dots), for each strain and time-point. Because data are left-skewed/not normally distributed, medians were chosen to approximate central tendency. Cells per cluster were measured by sampling strains over six days of growth, staining nuclei with DAPI, and imaging using fluorescent microscopy (xxxx). From left to right, time-points of maximum size for each strain were: 12, 12, 72, 120, 96, 108, 84, 72, 72, 96, 96, and 72 hours. From left to right, mean of median sizes (in cells per cluster) were: 1, 1, 1.4, 1.8, 1.8, 1.8, 4, 7.8, 5.4, 6.2, 5.6, and 5.6. Sizes at the initial time-point (0 hrs.) were omitted from analysis because they represent starting conditions. Shading is for ease of visualization.

Propagule Size

In order to determine propagule sizes of evolved strains, we manually analyzed 72-hour time-lapse videos and recorded the numbers of cells in propagules released from parent clusters. For most strains, the majority of propagules were single-celled, as observations

were skewed toward smaller propagules, which require less biomass to produce (Fig. 3, green dots). To accurately depict the context of individual cells in propagules, we also show the data as boxplots, weighted by biomass (Fig. 4, black boxplots). Strains that maintained ancestral characteristics and had the smallest average maximum cluster sizes (K1-01, K1-06, B5-06, B2-10, B2-12) released, almost exclusively, single-celled propagules. Although cells from strains B2-01 and B5-05 often exist in clusters, the vast majority of propagules released by these reproducing clusters were single-celled as well. In strains with larger average maximum cluster sizes that are maintained by encapsulation in maternal cells walls, as opposed to ECM, cells are more frequently released in multicellular propagules of up to 64 cells in size. Thus, among the strains that evolved under predation-selection, a variety of size-related traits emerged in both cluster size and propagule size.

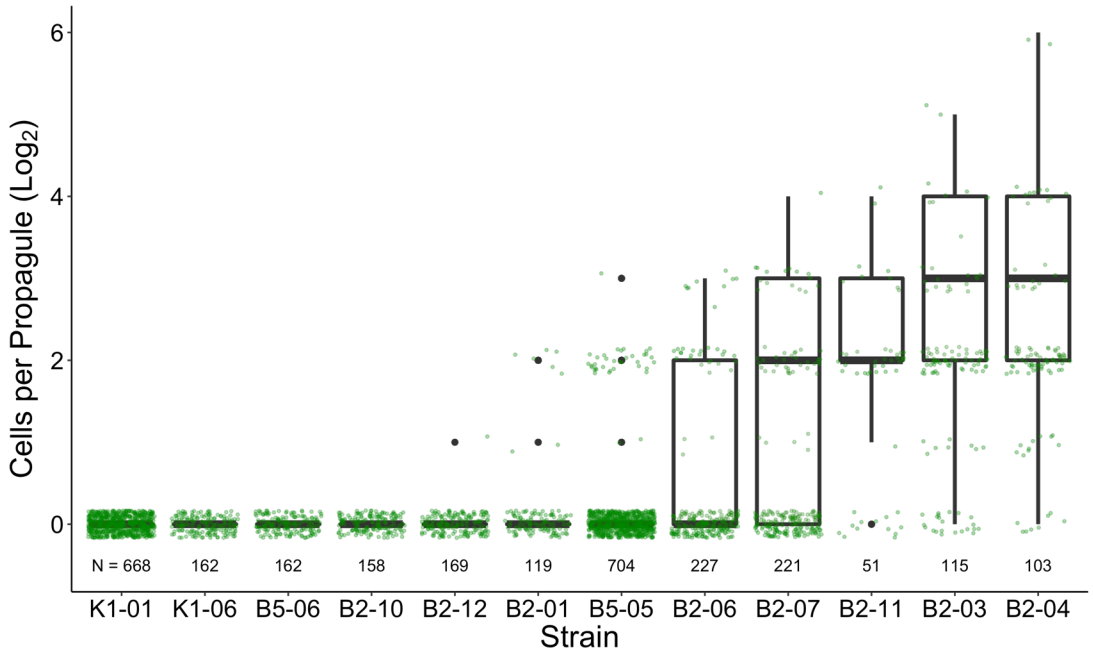

Figure 4. Sizes of propagules released by evolved strains during a 72-hour time-lapse. Propagule sizes were manually determined from time-lapse videos. Green dots show actual observations of propagule size. Because the frequency of observations is skewed toward smaller propagule sizes, we show the data as weighted boxplots as well, where a 32-celled propagule has 32 times the weight of a single-celled propagule. Sample sizes of propagule observations for each strain are indicated along the bottom of the plot. Strains ordered by weighted-mean propagule size.

Micrographic analysis using ImageJ revealed clear differences between the clustering behaviors of some populations. Experimental populations B1 and B4 showed negligible increases in clustering compared to the control (K) populations. Clones from population B2 showed a variety of clustering morphologies, with some clones above 90% clusters and some clones without any clusters at all. Similarly, population B3 showed a variety of clustering responses, but with a lower mean. All clones from population B5 showed an increase in clustering relative to the controls, with little variance.

Defense against predation

Multicellularity appears to provide an effective defense against predation. Comparisons were made by taking the absorbance value for each of the four replicates without predators and dividing by the average of the four replicates with predators. This value we label Δ_{abs}, and the resulting graph over the course of the experiment is shown in Figure 5. The unicellular strains, on average, experienced ~2.5-fold greater rates of predation compared to the multicellular strains. That is, the mean Δ_{abs} between hour 0 and hour 117 (day 5) were 0.367 and 0.140 for unicellular and multicellular strains respectively.

To simplify the analysis, inferences were drawn from the final time-point measurements (hour 117). A test for an effect of phenotype (unicellular or multicellular) on Δ_{abs} values shows that phenotype has a strong effect on algal density (ANOVA, $F_{1,22}$ = 8.65, P = 0.0076).

Because cells were mixed several times during the staining and imaging process, it is possible that some clusters of cells were disrupted. Thus, cluster sizes from fluorescent microscopy analysis are likely underestimates of cluster size, which may or

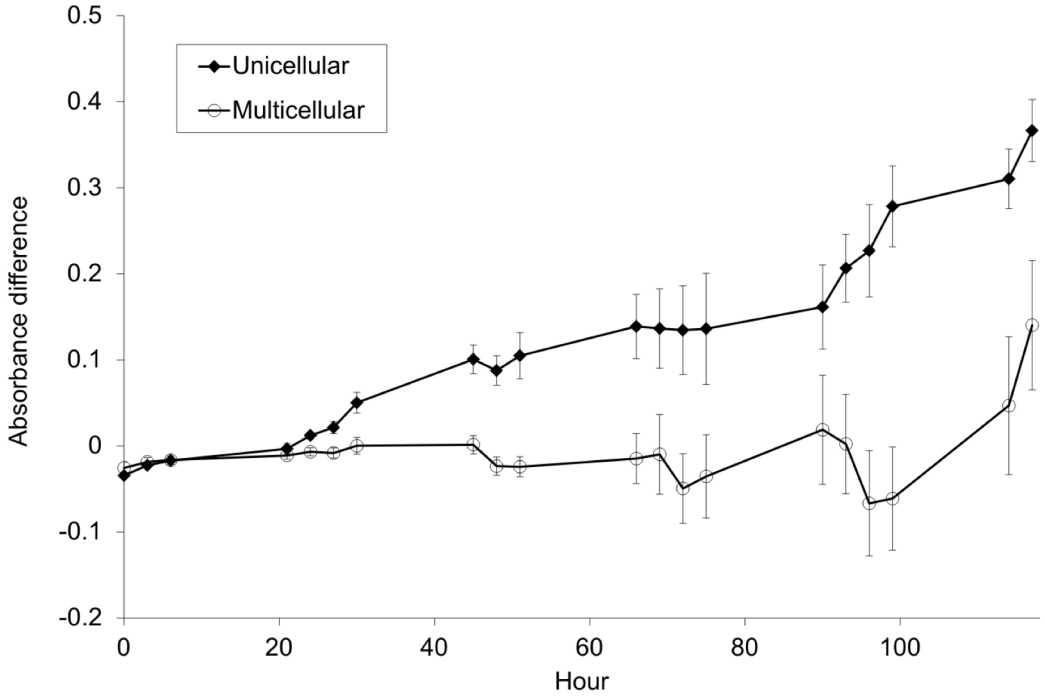

Figure 5. Δ_{abs} values for evolved multicellular and unicellular *C. reinhardtii* strains under predation. Multicellular strains averaged a much lower change in absorbance over the duration of the experiment than unicellular strains. Error bars are standard error of the mean for four technical replicates.

may not affect cluster size estimates for certain strains (i.e., those held together by extracellular matrix rather than the maternal cell wall) more than others.

Discussion

Our results show that the transition to a simple multicellular life cycle can happen rapidly in response to an ecologically relevant selective pressure. By increasing in size beyond the "predation threshold" (Kirk 1998 p. 55) of a filter-feeding predator, ancestrally unicellular *C. reinhardtii* are protected from predation for at least part of their life cycle. Under selection for increased size, formation of multicellular structures may be an easier route than increasing cell size because of trade-offs imposed by scaling relationships (primarily the reduction in surface area:volume ratio), because more mutational paths are available, and/or because available mutations have fewer or less severe pleiotropic effects.

Similar observations in other species suggest that the relative ease of transitioning to a multicellular life cycle is at least somewhat general. Such a transition has also occurred within 100 generations in the green alga *Chlorella vulgaris* (Boraas et al. 1998), and within 300 generations in the yeast *Saccharomyces cerevisiae* (Ratcliff et al. 2012). Although there have surely been many microbial evolution experiments in which multicellularity did not evolve, we can at least be confident that this phenomenon is not unique to *Chlamydomonas*. Grosberg and Strathmann (2007) may have been right to call the evolution of multicellularity a "minor major transition."

However, the available evidence also suggests a substantial stochastic component to the evolution of multicellularity. In previous experiments, multicellular structures evolved in one of ten selected populations in *C. reinhardtii* (Ratcliff et al. 2013) and in

"about 70%" of "many" selected populations in *C. vulgaris* (Boraas et al. 1998 p. 157). In the present experiment, multicellular structures evolved in two of five selected populations. Only in *S. cerevisiae* is the evolution of multicellular structures consistent across replicate populations (Ratcliff et al. 2012).

Comparisons between experiments, and between populations in this experiment, show that *C. reinhardtii* has multiple pathways available to evolve multicellularity. Under selection for an increased rate of settling out of liquid suspension, one population evolved multicellular structures held together by an extracellular matrix (Ratcliff et al. 2013), similar to those observed in isolate B2-01 in the present experiment (Fig. 2C). In both cases, unicellular propagules are released. In most isolates from population B2 in the present experiment (B2-02, B2-03, B2-04, B2-06, B2-07, B2-11), the multicellular phenotype results from a failure of daughter cells to break out of the mother cell wall (Fig 2D, E). The resulting propagules are either primarily multicellular or a mixture of unicellular and multicellular (Fig. 3).

Development in the isolates from population B2 is therefore strictly clonal, with important implications for evolvability. Since the cells within a multicellular structure are likely to be genetically identical, other than differences resulting from new mutations, genetic variation in a population would be partitioned primarily among colonies. The clonal development observed in these isolates therefore suggests that the observed multicellular clusters would be well-suited to serving as units of adaptation.

Even in the amorphous clusters observed in isolate B2-01 and those that evolved in response to selection for setting rate (Ratcliff et al. 2013), development is primarily clonal. Aggregation, through the incidental assimilation of free-swimming cells, was

occasionally observed in isolate B2-01. Although a similar process is possible in the life cycle that evolved in response to selection for setting rate (Ratcliff et al. 2013), it was not observed. Genetic conflicts among cells within clusters are therefore possible in these isolates, but their effects are likely to be minor.

In key respects, the isolates from population B2 appear to have recapitulated early steps in volvocine evolution; in fact, the evolved multicellular algae are similar in their gross morphology to small colonial volvocine algae such as *Pandorina*. However, we also find interesting differences between our experimental results and the ways in which multicellular volvocine algae are thought to have evolved in nature.

Comparisons of the evolved multicellular life cycle to that of wild-type, unicellular *C. reinhardtii* show that the mother cell wall is effectively acting as a colonial boundary.

The life cycle of wild-type *C. reinhardtii* includes a transient multicellular stage, between the division of the mother cell into (usually) two, four, or eight daughters and the rupture of the mother cell wall, which results in the release of those daughters into the external environment (Fig. 2A). In the evolved multicellular algae, the multicellular stage persists because the mother cell wall does not rupture until at least one additional round of cell division has occurred, resulting in the release of multicellular propagules (Fig. 2D, E). Furthermore, a degree of genetic control of cell number similar to that seen in undifferentiated colonial volvocine algae, manifests in our evolved multicellular strains. Propagules from the evolved multicellular strains were nearly all 4-, 8-, or 16-celled, a range similar to that of small colonial volvocine algae and smaller than that of *Pleodorina starrii,* in which propagules of a single genotype can span a 16-fold range of cell numbers (Herron et al. 2014).

Questions related to the emergence of multicellularity have traditionally been addressed through comparative studies of extant unicellular and multicellular lineages (King 2004; Kirk 2005; Herron and Michod 2008; Cock et al. 2010). Experimental evolution of *de novo* origins of multicellularity enables direct tests of hypotheses about this transition that could otherwise only be approached indirectly. The multicellular structures that have evolved in our experiments represent the very origins of multicellular development. Although the forms of multicellularity that have evolved are simple and apparently lacking in cellular differentiation, it is likely that most multicellular groups had similarly humble origins.

Our results support the view that predation may have played a role in at least some origins of multicellularity. Consistent with previous results, predation can drive the evolution of simple multicellular structures, and these structures provide protection from predators (Boraas et al. 1998; Becks et al. 2012). The 'chicken-and-egg' problem brought up by some authors – that multicellular predators are required to drive the evolution of multicellularity (e.g., Bonner 1998; Pentz et al. 2015) – does not exist: filter-feeding protists exist, including, for example, *Paramecium*, and there is no reason to think that such predators only arose after animals. Furthermore, some origins of multicellularity, including those of brown and volvocine algae, postdate that of animals, and could therefore have been driven by animal predation.

Acknowledgments

This work was supported by the National Science Foundation (DEB-1457701, DEB-1456652), the John Templeton Foundation (43285), the NASA Astrobiology Institute

(NNA17BB05A), a NASA Postdoctoral Program Fellowship to MDH, and a Packard Foundation Fellowship to WCR.

References

Becks, L., S. P. Ellner, L. E. Jones, and N. G. Hairston. 2010. Reduction of adaptive genetic diversity radically alters eco-evolutionary community dynamics. Ecol. Lett. 13:989–997.

Becks, L., S. P. Ellner, L. E. Jones, and N. G. Hairston. 2012. The functional genomics of an eco-evolutionary feedback loop: linking gene expression, trait evolution, and community dynamics. Ecol. Lett. 15:492–501.

Bell, G. 1985. The origin and early evolution of germ cells as illustrated by the Volvocales. Alan R. Liss, New York.

Bonner, J. T. 1998. The origins of multicellularity. Integr. Biol. 1:27–36.

Boraas, M. E., D. B. Seale, and J. E. Boxhorn. 1998. Phagotrophy by a flagellate selects for colonial prey: a possible origin of multicellularity. Evol. Ecol. 12:153–164.

Buss, L. W. 1987. The Evolution of Individuality. Princeton University Press, Princeton.

Butterfield, N. J. 2000. *Bangiomorpha pubescens* n. gen., n. sp.: implications for the evolution of sex, multicellularity, and the Mesoproterozoic/Neoproterozoic radiation of eukaryotes. Paleobiology 26:386–404.

Cock, J. M., L. Sterck, P. Rouzé, D. Scornet, A. E. Allen, G. Amoutzias, V. Anthouard, F. Artiguenave, J.-M. Aury, J. H. Badger, B. Beszteri, K. Billiau, E. Bonnet, J. H. Bothwell, C. Bowler, C. Boyen, C. Brownlee, C. J. Carrano, B. Charrier, G. Y. Cho, S. M. Coelho, J. Collén, E. Corre, C. Da Silva, L. Delage, N. Delaroque, S. M.

Dittami, S. Doulbeau, M. Elias, G. Farnham, C. M. M. Gachon, B. Gschloessl, S. Heesch, K. Jabbari, C. Jubin, H. Kawai, K. Kimura, B. Kloareg, F. C. Küpper, D. Lang, A. Le Bail, C. Leblanc, P. Lerouge, M. Lohr, P. J. Lopez, C. Martens, F. Maumus, G. Michel, D. Miranda-Saavedra, J. Morales, H. Moreau, T. Motomura, C. Nagasato, C. A. Napoli, D. R. Nelson, P. Nyvall-Collén, A. F. Peters, C. Pommier, P. Potin, J. Poulain, H. Quesneville, B. Read, S. A. Rensing, A. Ritter, S. Rousvoal, M. Samanta, G. Samson, D. C. Schroeder, B. Ségurens, M. Strittmatter, T. Tonon, J. W. Tregear, K. Valentin, P. von Dassow, T. Yamagishi, Y. Van De Peer, and P. Wincker. 2010. The Ectocarpus genome and the independent evolution of multicellularity in brown algae. Nature 465:617–621. Nature Publishing Group, a division of Macmillan Publishers Limited. All Rights Reserved.

Gorman, D. S., and R. P. Levine. 1965. Cytochrome F and plastocyanin: their sequence in the photosynthetic electron transport chain of Chlamydomonas reinhardtii. Proc. Natl. Acad. Sci. USA 54:1665–1669.

Grosberg, R. K., and R. R. Strathmann. 2007. The evolution of multicellularity: a minor major transition? Annu. Rev. Ecol. Evol. Syst. 38:621–654.

Guillard, R. R. L. 1975. Culture of phytoplankton for feeding marine invertebrates. Pp. 29–60 *in* W. L. Smith and M. H. Chantey, eds. Culture of Marine Invertebrate Animals. Plenum Publishers, New York.

Harris, E. H. 2009. The Chlamydomonas Sourcebook, Second Edition. Academic Press, San Diego, California.

Herron, M. D., S. Ghimire, C. R. Vinikoor, and R. E. Michod. 2014. Fitness trade-offs and developmental constraints in the evolution of soma: an experimental study in a

volvocine alga. Evol. Ecol. Res. 16:203–221.

Herron, M. D., and R. E. Michod. 2008. Evolution of complexity in the volvocine algae: transitions in individuality through Darwin's eye. Evolution 62:436–451.

Herron, M. D., A. Rashidi, D. E. Shelton, and W. W. Driscoll. 2013. Cellular differentiation and individuality in the "minor" multicellular taxa. Biol. Rev. Camb. Philos. Soc. 88:844–861.

Kaiser, D. 2001. Building a multicellular organism. Annu. Rev. Genet. 35:103–23. Annual Reviews 4139 El Camino Way, P.O. Box 10139, Palo Alto, CA 94303-0139, USA.

Kilham, S. S., D. A. Kreeger, S. G. Lynn, C. E. Goulden, and L. Herrera. 1998. COMBO: A defined freshwater culture medium for algae and zooplankton. Hydrobiologia 377:147–159.

King, N. 2004. The unicellular ancestry of animal development. Dev. Cell 7:313–325.

King, N., C. T. Hittinger, and S. B. Carroll. 2003. Evolution of key cell signaling and adhesion protein families predates animal origins. Science 301:361–363.

Kirk, D. L. 2005. A twelve-step program for evolving multicellularity and a division of labor. BioEssays 27:299–310.

Kirk, D. L. 1998. Volvox: Molecular-Genetic Origins of Multicellularity. Cambridge University Press, Cambridge.

Leliaert, F., D. R. Smith, H. Moreau, M. D. Herron, H. Verbruggen, C. F. Delwiche, and O. De Clerck. 2012. Phylogeny and molecular evolution of the green algae. CRC. Crit. Rev. Plant Sci. 31:1–46.

Pentz, J. T., T. Limberg, N. Beermann, and W. C. Ratcliff. 2015. Predator escape: an

ecologically realistic scenario for the evolutionary origins of multicellularity. Evol. Educ. Outreach 8:13. Springer US.

R Development Core Team. 2009. R: A Language and Environment for Statistical Computing. R Foundation for Statistical Computing, Vienna, Austria.

Ratcliff, W. C., R. F. Denison, M. Borrello, and M. Travisano. 2012. Experimental evolution of multicellularity. Proc. Natl. Acad. Sci. USA 109:1595–1600.

Ratcliff, W. C., M. D. Herron, K. Howell, J. T. Pentz, F. Rosenzweig, and M. Travisano. 2013. Experimental evolution of an alternating uni- and multicellular life cycle in *Chlamydomonas reinhardtii*. Nat. Commun. 4:2742.

Schindelin, J., I. Arganda-Carreras, E. Frise, V. Kaynig, M. Longair, T. Pietzsch, S. Preibisch, C. Rueden, S. Saalfeld, B. Schmid, J.-Y. Tinevez, D. J. White, V. Hartenstein, K. Eliceiri, P. Tomancak, and A. Cardona. 2012. Fiji: an open-source platform for biological-image analysis. Nat. Methods 9:676–682.

Stanley, S. M. 1973. An ecological theory for the sudden origin of multicellular life in the Late Precambrian. Proc. Natl. Acad. Sci. USA 70:1486–1489.

Suga, K., Y. Tanaka, Y. Sakakura, and A. Hagiwara. 2011. Axenic culture of Brachionus plicatilis using antibiotics. Hydrobiologia 662:113–119.